ELSEVIER

Molecular Brain Research 26 (1994) 26–36

MOLECULAR BRAIN RESEARCH

Research Report

Expression of the growth-associated protein B-50/GAP43 via a defective herpes-simplex virus vector results in profound morphological changes in non-neuronal cells

J. Verhaagen [a,*], W.T.J.M.C. Hermens [a,1], A.B. Oestreicher [a], W.H. Gispen [a], S.D. Rabkin [b], D.W. Pfaff [c], M.G. Kaplitt [c]

[a] *Rudolf Magnus Institute, Department of Medical Pharmacology, Vondellaan 6, 3521 GD Utrecht, The Netherlands*
[b] *Georgetown University Medical Center, Department of Neurosurgery, 3800 Reservoir Road NW, Washington DC, 20007, USA*
[c] *The Rockefeller University, Laboratory of Neurobiology and Behavior, 1230 York Avenue, New York, NY, 10021, USA*

Accepted 19 April 1994

Abstract

This study describes the creation and application of a defective herpes simplex viral (HSV) vector for B-50/GAP-43, a neural growth-associated phosphoprotein. We demonstrate abundant expression of B-50/GAP-43 in cultured non-neuronal cells (African green monkey kidney cells [vero cells] and Rabbit skin cells) via this HSV vector. When B-50/GAP-43 was expressed in non-neuronal cells major morphological changes occurred that included extensive membrane ruffling, the formation of filopodia and long thin extensions reminiscent of neurites. These extensions often terminated in growth cone-like structures. Quantitation of these morphological changes at different times following infection demonstrates that the surface area of the B-50/GAP-43-expressing cells started to increase between 6 and 10 h post-infection. At 72 h, B-50/GAP-43-positive cells were 3.0 times larger in size and one third of the cells expressed long processes with a mean length of 165 ± 14.5 μm. Ultrastructural studies of cells 48 h after infection revealed that B-50/GAP-43 is predominantly localized at the plasma membrane of the elaborated processes. Some immunoreactivity was associated with vesicular structures that appear to be in-transit in the processes. These observations suggest that B-50/GAP-43 acts at the plasmamembrane to induce a neuron-like morphology in non-neuronal cells persisting for several days in culture. In the future the defective viral vector will enable gene transfer to express B-50/GAP-43 in neurons in vivo in order to study its involvement in regenerative sprouting and neuroplasticity.

Keywords: Growth-associated protein B-50/GAP-43; Defective herpes simplex vector; Gene transfer; Process formation

1. Introduction

Adult nervous systems consist of complex neuronal networks. The initiation of nerve fiber formation is one of the first crucial events in an elaborate process eventually resulting in the establishment of these highly organized structures. The regulation of nerve fiber growth is under the control of extracellular molecules including growth factors, cell adhesion molecules and extracellular matrix components. In addition a number of proteins have been implicated in the intracellular mechanisms that regulate neurite outgrowth. These include the cytoskeletal protein actin [26,46], juvenile forms of tubulin [28,13], microtubule-associated proteins [8,27], the developmentally regulated dendritic protein Drebrin [35], and the growth-associated protein B-50/GAP-43 [10,40].

GAP43 was originally discovered in an attempt to identify proteins specifically transported into growing axons [5,37]. Earlier, a substrate of protein kinase C was isolated which was specific to nervous tissue and this protein was called B-50 [23,58,59]. Subsequently molecular cloning revealed that GAP-43 [4] and B-50

* Corresponding author. Present address: Netherlands Institute for Brain Research, Meibergdreef 33, 1105 AZ Amsterdam, The Netherlands. Fax: (31) 20-696 1006.

[1] Present address: Netherlands Institute for Brain Research, Meibergdreef 33, 1105 AZ Amsterdam, The Netherlands. Fax: (31) 20-696 1006.

SSDI 0169-328X(94)00092-S

[29] are the same protein and are also homologous to F1 [32], a protein associated with long-term potentiation and neuromodulin, a calmodulin-binding protein [9]. An intense interest developed in determining what role, if any, B-50/GAP-43 plays in the development and regeneration of nerve fibers.

Studies on the localization and the regulation of B-50/GAP-43 protein expression and transport have yielded some insights in the role of this protein in axonal growth. The abundance of B-50/GAP-43 in the growth cone [11,20,39] and in developing embryonic neurons [6], coupled with a downregulation of the expression of the protein shortly following target cell innervation has furthered speculation that B-50/GAP-43 actively participates in the regulation of nerve fiber outgrowth [40]. B-50/GAP-43 levels in injured peripheral nervous system (PNS) neurons are normally upregulated following a lesion and increased levels of B-50/GAP43 are associated with periods of nerve regeneration [19,37,38,49,52]. The decline in B-50/GAP43 closely correlates with the completion of synapse formation and with the maturation of axon–glia interactions. This suggests that inhibitory signals associated with these events may play a role in down-regulating B-50/GAP-43 expression and that injury may interrupt this inhibitory influence resulting in reinduction of B-50/GAP-43 expression [41].

Despite the close correlation between B-50/GAP-43 expression and axonal growth, the precise role of this protein remains elusive. B-50/GAP-43 expression in cultured hippocampal neurons precedes the determination of neuronal polarity [50]. During the initial stages of nerve fiber elongation B-50/GAP-43 is equally distributed in all short processes and their growth cones. As polarity in these cultured neurons develops B-50/GAP-43 becomes more abundant in the faster growing axonal process [16,50]. In PC-12 cells, treatment with nerve growth factor (NGF) results in a redistribution of B-50/GAP-43 from vesicular structures in the cytosol to the plasma membrane [51]. This occurs coincident with the initiation of nerve fiber outgrowth during neuronal differentiation of this cell line. Some of the most direct evidence supporting a role for B-50/GAP-43 in the determination of process outgrowth and cell shape has been obtained in experiments in which the levels of B-50/GAP-43 were manipulated in cell lines. Non-neuronal cells that express B-50/GAP-43 exhibit transient cell surface reactions during the first hours following plating of the cell [55,57]. Stable transfection of neuroblastoma cell lines resulted in more rapid neurite outgrowth in response to differentiating stimuli [30,56] and a longer maintenance of formed processes on withdrawal of such signal [24]. Downregulation of B-50/GAP-43 expression with anti-sense B-50/GAP-43 oligonucleotides or blocking of B-50/GAP-43 with anti-B-50/GAP-43 antibodies results in a diminished outgrowth response in neuroblastoma cells [36,19].

The purpose of this study was to develop a defective herpes simplex virus (HSV) vector which would result in high-level long-term expression of B-50/GAP-43 in mammalian cells in vitro and in vivo. The defective viral vector system used is a plasmid based vector containing two HSV recognition sequences, the cleavage/packaging signal and the origin of replication, which allows packaging of the plasmid in cells in tissue culture in the presence of viral proteins supplied by a helper virus [25,42]. Defective viral vectors have been used successfully to direct in-vitro and in-vivo expression of genes in neurons [14,15,17,21,22]. We employed these viral vectors to direct high-level sustained expression of B-50/GAP-43 to non-neuronal cells (Vero-type African green monkey kidney cells and rabbit skin cells) and observed the induction of long neurite-like processes and structures reminiscent of growth cones. In contrast to the previously reported transient changes in cell shape observed during the first hours following plating of B-50/GAP-43 expressing non-neuronal cells [55,57] the present morphological changes persisted for several days in culture. Furthermore, we report the induction of much longer processes than previously observed. Our observations support the notion that B-50/GAP-43 is directly involved in the initiation and maintenance of nerve fiber growth.

2. Materials and methods

2.1. Construction of amplicons

The construction of amplicon pHCL containing the bacterial *lacZ* gene under the control of the human Cytomegalovirus immediate early (CMV) promoter has been described previously [21]. The amplicon pHCB-50 (Fig. 1) was generated as follows. *Sal*I restriction sites were introduced 5′ and 3′ of the CMV-promoter – SV-40 poly(A) signal expression cassette of pcDNA I (Invitrogen) using the polymerase chain reaction (PCR). The PCR product was digested with *Sal*I, gel-purified and ligated in the *Sal*I site of pGEM2 (Promega) resulting in pGEM-CMV. An *Eag*I and *Sma*I site were introduced 5′ and 3′ of the rat B-50 coding sequence directly adjacent of the translation start and stop codons using the B-50 cDNA [29] as a template. The PCR product was digested with *Eag*I and *Sma*I and cloned downstream of the CMV promotor in the *Eag*I and *Eco*RV sites of pGEM-CMV resulting in pGEM-CMV-B-50. The B-50 coding sequence in pGEM-CMV-B-50 was sequenced. This revealed no PCR errors or cloning artifacts. pGEM-CMV-B-50 was digested with *Sal*I and the CMV-B50-poly(A) fragment was cloned into the unique *Sal*I site of pSRa-ori, a plasmid containing the HSV-1 cleavage/packaging signal and HSV-2 origin of replication [21]. This yielded amplicon pHCB-50 (Fig. 1).

2.2. Tissue culture and generation of defective viral vectors

Tissue culture media and reagents were from Gibco. Vero (African green monkey kidney) cells were obtained from the American Tissue-type Culture Collection and rabbit skin cells were obtained

from Dr. Ann Kwong. These cell lines were maintained in Dulbecco's modified Earle's medium (DMEM) containing 10% inactivated fetal calf serum (IFCS) at 37°C in an atmosphere of 5% CO_2. For the production of virus stocks, Vero cells were plated and allowed to grow to confluence in T150 tissue culture flasks (Nunc). Defective viral particles were generated as described previously [21] using a temperature-sensitive mutant helper virus (tsK) obtained from J. Subak-Sharpe, Institute of Virology (Glasgow, Scotland). Defective viral titers were determined by histochemical staining for β-gal or by immunohistochemistry for B-50/GAP-43 as described below. Viral stocks were devoid of wildtype virus since no plaque formation occurred at 39°C in infected cultures.

2.3. Infection of cells with defective viral vectors

To analyse the B-50/GAP-43 protein product synthesized via dvHCB-50 and to study the effect of B-50/GAP-43 on cellular morphology, cells were cultured at densities of 2×10^4 cells per cm^2 on poly-L-lysine (Sigma) coated microscope slides (26×40 mm) in DMEM with 10% IFCS. Cells were allowed to grow for 6 to 72 h following plating and were infected with 1.5 μl of concentrated virus (m.o.i. = 0.02) diluted in 1 ml phosphate-buffered saline (PBS, pH 7.4)/1% IFCS per microscope slide. One and a half hour later the virus containing buffer was removed and fresh DMEM/10% IFCS was added to the cells. The cells were allowed to grow for 6 to 72 h at 39°C and were subsequently processed for Western blotting or light and electron microscopy.

2.4. Gel electrophoresis and immunoblotting

For Western blot analysis, B-50/GAP-43 infected Vero cells were removed from the microscope slide at 24 and 48 h following infection using a denaturing electrophoresis sample buffer [58]. Prior to electrophoresis, proteins in sample buffer were heated for 10 min at 80°C. Proteins were separated by sodium dodecyl sulfate–polyacrylamide gel electrophoresis [58] and separated proteins were transferred from the 11% gels to nitrocellulose [48], immunostaining of the blots with affinity-purified anti-B-50/GAP-43 antibody derived from antiserum #8921 [31] was performed under standard conditions [53].

2.5. Light microscopy

Cells in 12-well microtiter plates (for the determination of the titers of the viral stocks) or cells cultured on poly-L-lysine-coated microscope slides (to study effects of B-50/GAP-43 on morphology) were fixed for 15 min in 4% paraformaldehyde in 0.1 M phosphate buffer at pH 7.4 (PB). Following fixation, cells were rinsed extensively with PBS. β-Galactosidase expressing cells were visualized with a standard histochemical staining procedure using X-gal as a substrate [33]. B-50 was detected with affinity-purified polyclonal rabbit antibodies (dilution 1:2500). All incubations with antibody were at room temperature in PBS containing 0.1% Triton X-100 and 0.2% BSA. After each incubation with antibody, cells were washed with PBS/0.1% Triton X-100. Primary antibody incubations were performed overnight. Antigen–antibody binding was visualized with biotinylated secondary antibodies and an avidin/biotin/HRP staining kit (Vector laboratories, Burlingame, CA) according to the procedure supplied with the kit. Immunostained cells were briefly counterstained with hematoxylin, dehydrated, embedded in Depex mounting medium and examined in an Olympus BH-2 microscope.

2.6. Quantification of cell shape

For each cell, the surface area, the number of cellular extensions and the length of the extensions were determined with a computerized image analysis system (DIFA, Breda, The Netherlands). To this end cells were visualized on a television screen with a 20× objective using an Olympus BH-2 microscope equipped with a videocamera linked to an IBM computer. To avoid biased sampling three randomly chosen fields were marked with a pencil on each slide by an investigator not directly involved in the quantification (J.V.) and the cells present in these field were analysed (by W.T.J.M.C.H.). Thirty to 59 β-gal and B-50/GAP-43 cells were analysed at 6, 10, 24, 48 and 72 h post-infection.

2.7. Electron microscopy

Vero cells cultured on poly-L-lysine-coated thermanox coverslips were fixed in 4% paraformaldehyde/2% glutaraldehyde (biological grade, Polysciences, Warrington, USA) in PB for 20 min at 4°C. Fixed cells were washed in PB and aldehyde groups were inactivated in a freshly prepared solution of sodium borohydride and 0.1% glycine in PB. Before and after each immuno-incubation, cells were rinsed for 1 h in 0.5% BSA and 0.1% gelatin in PB. This solution was also used as diluent of the primary and secondary antibodies and as incubation medium of the primary antibody which also contained 0.1% saponin and 2% normal goat serum. Cells were incubated overnight in 1:300 diluted affinity-purified anti-B-50/GAP-43 antibodies. The next morning, cells were rinsed for 2 h and incubated in 1:80 diluted goat anti-rabbit immunoglobulines conjugated to 1 nm gold particles (Aurion, Wageningen, NL) for 5 h at 37°C. The cells were subsequently rinsed for 1 h in 0.5% BSA and 0.1% gelatin in PB and in PB, fixed for 10 min in 2.5% glutaraldehyde in PB, washed in PB and incubated in 0.1% osmium tetroxide in PB for 30 min. After 3 rinses of 3 min, each in deionized water the cells were treated according the *N*-propyl-gallate silver enhancement method [3]. Thereafter, Vero cells were rinsed and stored temporarily in PB. Subsequently, cells were rinsed 3 times, fixed in 2% uranyl acetate in 50% ethanol for 30 min and dehydrated and embedded in epon. Thermanox coverslips were removed from the resin, leaving the cells at the surface of the epon block. Ultrathin sections of the epon embedded cells were prepared with a Reichert-Jung Ultracut microtome, mounted on formfar-coated nickel grids and the sections were photographed without counter staining in a Philips CM10 electron microscope [50].

3. Results

3.1. Creation of B-50/GAP-43 amplicons and generation of defective viral vector

Amplicon pHCB-50 is based on a previously described prototype, pSRa-ori [21]. This plasmid contains the HSV cleavage packaging signal ('a' sequence) and origin of replication. The B-50/GAP-43 coding region was placed under the control of the CMV promoter with the SV40 poly-adenylation signal downstream of the coding region. This transcription unit was inserted into pSRa-ori creating pHCB-50 (Fig. 1). Following transfection of amplicons pHCB-50 and pHCL (an amplicon containing a transcription unit for lacZ and constructed by Kaplitt et al. [21]) into rabbit skin cells, defective HSV vectors were created by superinfection with the temperature-sensitive helper virus tsK, which replicates at 31°C but is inactive at 39°C. The resulting viral stocks were serially passaged and the helper and

defective titers were determined for each passage as described in the Materials and Methods section. Titers of viral stocks were 3.6×10^6 (dvHCL) and 5.9×10^6 (dvHCB-50) infectious defective viral particles per ml and 1.2×10^6 (dvHCL) and 1.9×10^6 (dvHCB-50) plaque forming units of tsK helper virus per ml. For titering immunohistochemistry was used to detect expression of B-50/GAP-43 protein and enzyme histochemistry was used to detect β-galactosidase 24 h following infection. Positive cells were clearly identified in plates infected with dilutions of the viral vector dvHCB-50. Uninfected cells, as well as cells infected with helper virus alone or with the *lacZ*-expressing virus dvHCL were completely negative for B-50/GAP-43. In addition the number of B-50/GAP-43-positive cells changed proportionately to the viral dilution factor, thereby confirming that the positive cells were the result of a viral infection. This demonstrates that B-50/GAP-43 protein expression was the result of expression from defective viral vector dvHCB-50 (data not shown).

To determine if infection of Vero cells results in the expression of intact B-50/GAP-43, a Western blot with proteins extracted from dvHCB-50-infected Vero cells, non-infected Vero cells and from mouse brain was incubated with B-50/GAP-43 antibody. Expression of

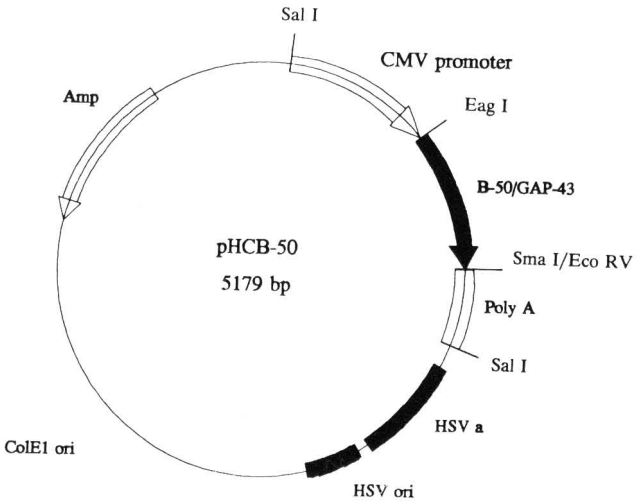

Fig. 1. Diagram of B-50/GAP-43 amplicon pHCB-50. pHCB-50 is based on amplicon pSRaori (Kaplitt et al. [21]) and contains the B-50/GAP-43 coding sequence under the control of the CMV promoter. An SV40 polyadenylation signal (polyA) is located downstream of the transcription unit. The entire transcription unit was inserted in a unique *Sal*I restriction site in the polylinker of pSRa-ori. The *Eag*I and *Sma*I/*Eco*RV site used to insert the B-50/GAP-43-coding sequence is indicated. The position of the HSV cleavage/packaging signal (HSV a), the HSV origin of replication (HSV ori), the ampicilin resistance gene (Amp) and the ColE1 ori are indicated. In the presence of the HSV proteins provided by the helper virus, the HSV ori allows replication of the amplicon and the HSV a sequence permits cleavage of 150kb length units of DNA and packaging into HSV virions.

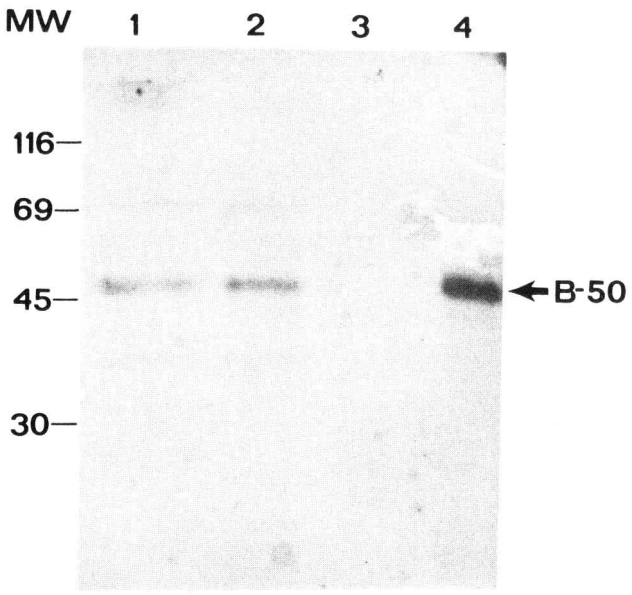

Fig. 2. Analysis of B-50/GAP-43 protein expression from dvHCB-50. A Western blot prepared from vero cell proteins extracted 24 (lane 1) and 48 (lane 2) h after infection with dvHCB-50 and proteins from non-infected Vero cells (lane 3) and from mouse brain (lane 4) was incubated with anti-B-50/GAP43 antibody. Each sample contained 70 μg of total protein. The B-50/GAP-43 immunoband in dvHCB-50 infected Vero cell extracts runs at the same position as B-50/GAP-43 in a protein extract from mouse brain. This demonstrates that the expression of B-50/GAP-43 in Vero cells via dvHCB-50 results in the synthesis of intact B-50/GAP-43. The position of molecular weight markers is indicated on the left.

B-50/GAP-43 is readily detectable in infected Vero cells but is absent from non-infected cells. B-50/GAP-43 expressed in Vero cells via dvHCB-50 migrates in Western blots to the same position as B-50/GAP-43 from mouse brain (Fig. 2).

3.2. Effect of B-50 / GAP-43 on the morphology of non-neuronal cells

Vero cells at a culture density of 2×10^4 cells/cm^2 (covering approximately 20% of the microscope slide) were infected with dvHCB-50 or with dvHCL and their morphology was studied at 6, 10, 24, 48 and 72 h post-infection. Visual inspection of dvHCB-50-infected Vero cells revealed the occurrence of striking changes in the morphology of the B-50/GAP-43-immunoreactive cells in a time-dependent fashion. Such changes were not observed in the β-gal-positive cells (Fig. 3). At 10 h after infection, B-50/GAP-43-positive cells were significantly larger in size than the β-gal cells. At this time point, most B-50/GAP-43-positive cells exhibited irregular membranes but no long processes were observed yet. At 24, 48 and 72 h post-infection, two distinct phenotypes were apparent (Fig. 3): (1) virtually all B-50/GAP-43 cells were larger in size than the cells expressing β-gal and exhibited ruffled mem-

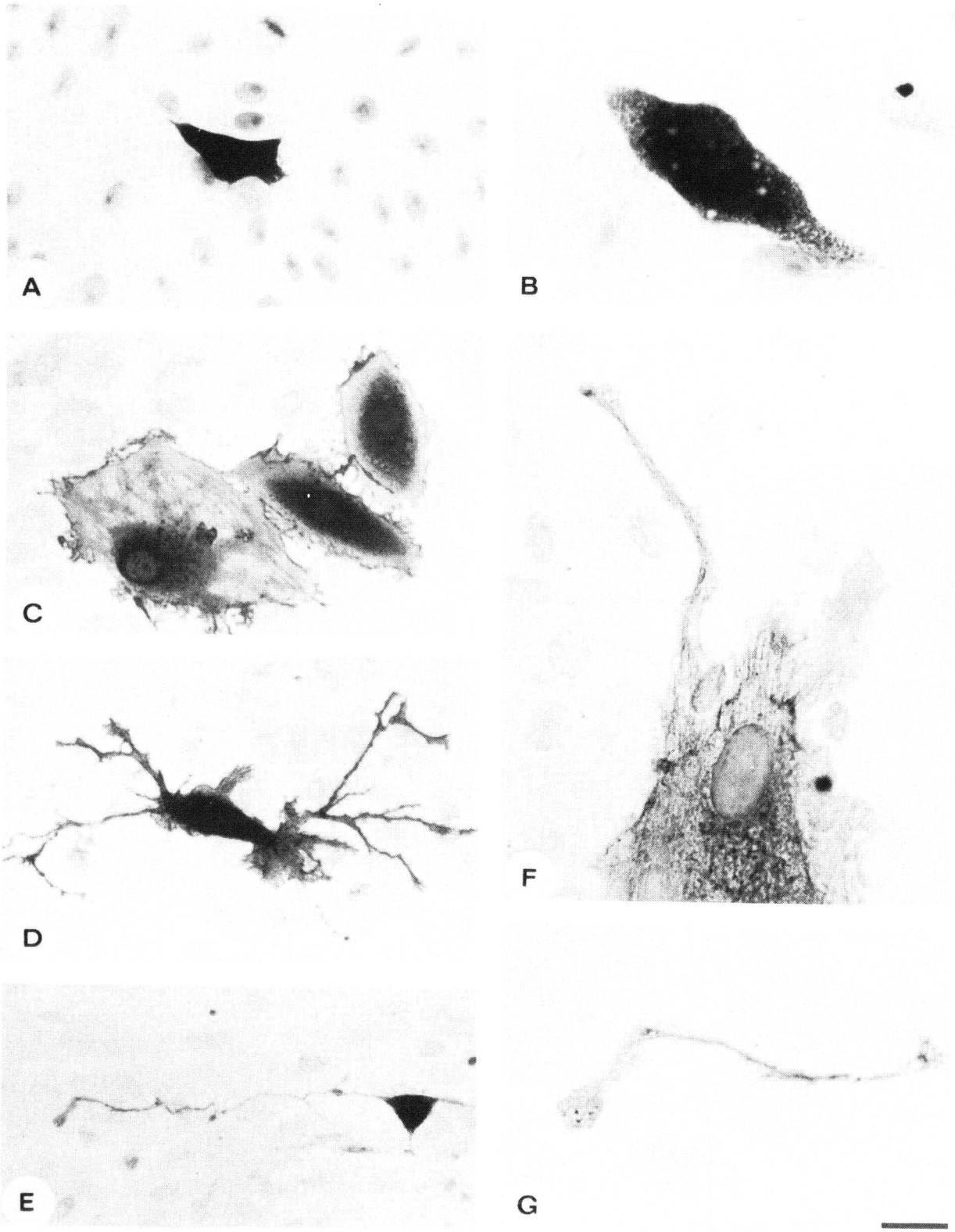

Fig. 3. Comparison of the morpholgy of Vero cells infected with dvHCL and dvHCB-50. At various timepoints following infection with defective viral vectors cells were fixed and β-gal or B-50/GAP-43 expression was visualized with a histochemical staining (β-gal) or by immunohistochemistry (B-50/GAP-43). A,B: Vero cells expressing β-gal 48 h after infection with dvHCL. C,D,E,F,G: Vero cells expressing B-50/GAP-43 48 h (C,E,F,G) and 72 h (D) after infection with dvHCB-50. B-50/GAP-43 expression results in enlarged cells with ruffled membranes and numerous filopodia (C) or in cells with long thin processes (D,E,F). Details of Vero cells in F and G illustrate growth cone-like structures on B-50/GAP-43 expressing cells. G is a magnification of the process in E. Changes such as shown here were observed in nearly all cells expressing B-50/GAP-43 between 24 and 72 h following infection in 4 independent experiments. In contrast no such changes were seen in cells expressing B-50/GAP-43 at 6 h post-infection or in β-gal expressing cells throughout the 72 h observation period. Bar = 50 μm (for A,C,D,E) and 19 μm for (B,F,G).

branes and filopodial-like extensions, (2) a second class of cells exhibited additional long processes (a process is defined as an extension longer than 15 μm) often terminating in club-shaped growth cone-like structures. First-order processes emanating directly from the cell surface occasionally branched to form second-order

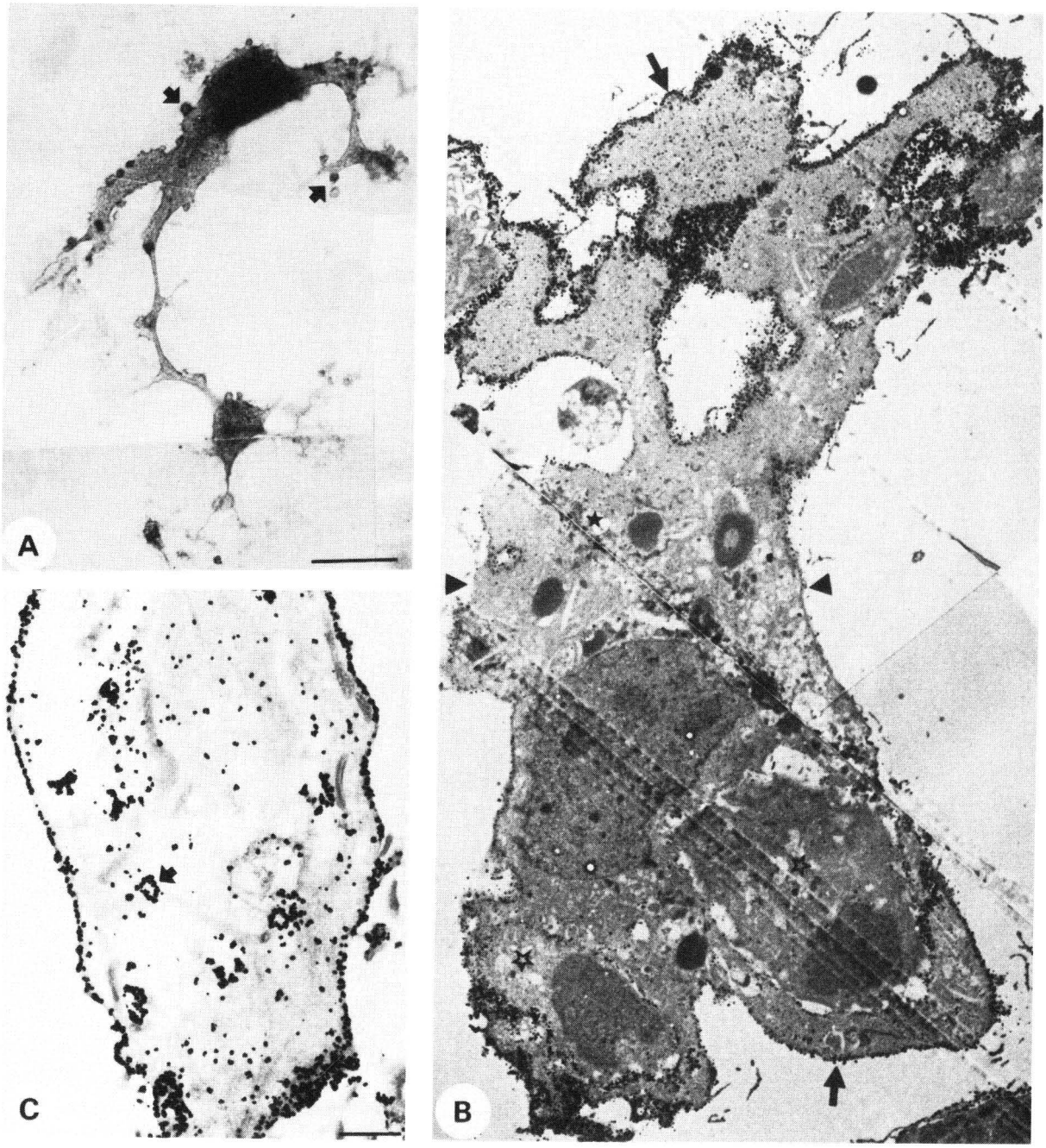

Fig. 4. Examples of varicosities on B-50/GAP-43-expressing Vero cells and ultrastructural localization of B-50/GAP-43 48 h following infection with dvHCB-50. A: in some Vero cells high local concentrations of B-50/GAP-43 (arrows) are observe at the plasma membrane of cellular processes. Note that these foci of high B-50 expression are often associated with varicosities and 50 μm (for B and C). B,C: ultrastructural localization of B-50/GAP-43 in dvHCB-50-infected Vero cells. Cells were processed for immuno-electron microscopy and the localization of B-50/GAP-43 was visualized with an immunogold labelling techniques using silver enhancement as described in Materials and methods. B illustrates the ultrastructural localization of B-50/GAP-43 in a Vero cell extending processes. The cell body of the immunolabelled Vero cell is indicated by a solid asterisk and the cell body plasma membrane is indicated by arrowheads. Two non-labelled Vero cells are indicated by an open asterix. Note that the B-50/GAP-43-positive cell is much larger then the non-labelled cells and that the immunogold labelling is predominantly present on the plasma membrane of the extensions (arrows) and is much lower on the plasma membrane of the cell body (arrowhead). The two non-labelled Vero cells appear to be engulfed by the processes formed on the B-50/GAP-43 expressing cell. C shows an ultrastructural detail of a B-50/GAP-43-labelled Vero cell extension. Note that the immunolabelling is associated with the plasma membrane and with vesicular structures in the process. Bar in A = 19 μm. Bar in B = 3.3 μm for B and 1 μm for C.

extensions (Fig. 3D,F,G). In both phenotypes, swellings along the plasma membrane resembling varicosities were present usually containing high levels of B-50/GAP-43 (Fig. 4A). The morphological changes in B-50/GAP-43-expressing Vero cells were seen in 4 independent experiments. In addition, similar changes in cell shape were observed in another non-neuronal cell line, rabbit skin cells. The changes in these cells were only investigated at 48 h after infection but were comparable to the morphological effects seen in the Vero cells (Fig. 5).

For the ultrastructural studies, sections of transfected Vero cells were selected and examined in which both the cell body and extending processes could be observed. Fig. 4B shows that B-50/GAP-43 was predominantly localized at the plasma membrane of the Vero cell processes. The plasma membrane of the cell body was also immunolabelled but to a much lesser extent then the extensions. Some immunolabelling in the cytoplasm was associated with vesicular structures that might be in-transit (Fig. 4C). B-50/GAP-43-immunolabelled processes were often in intimate contact

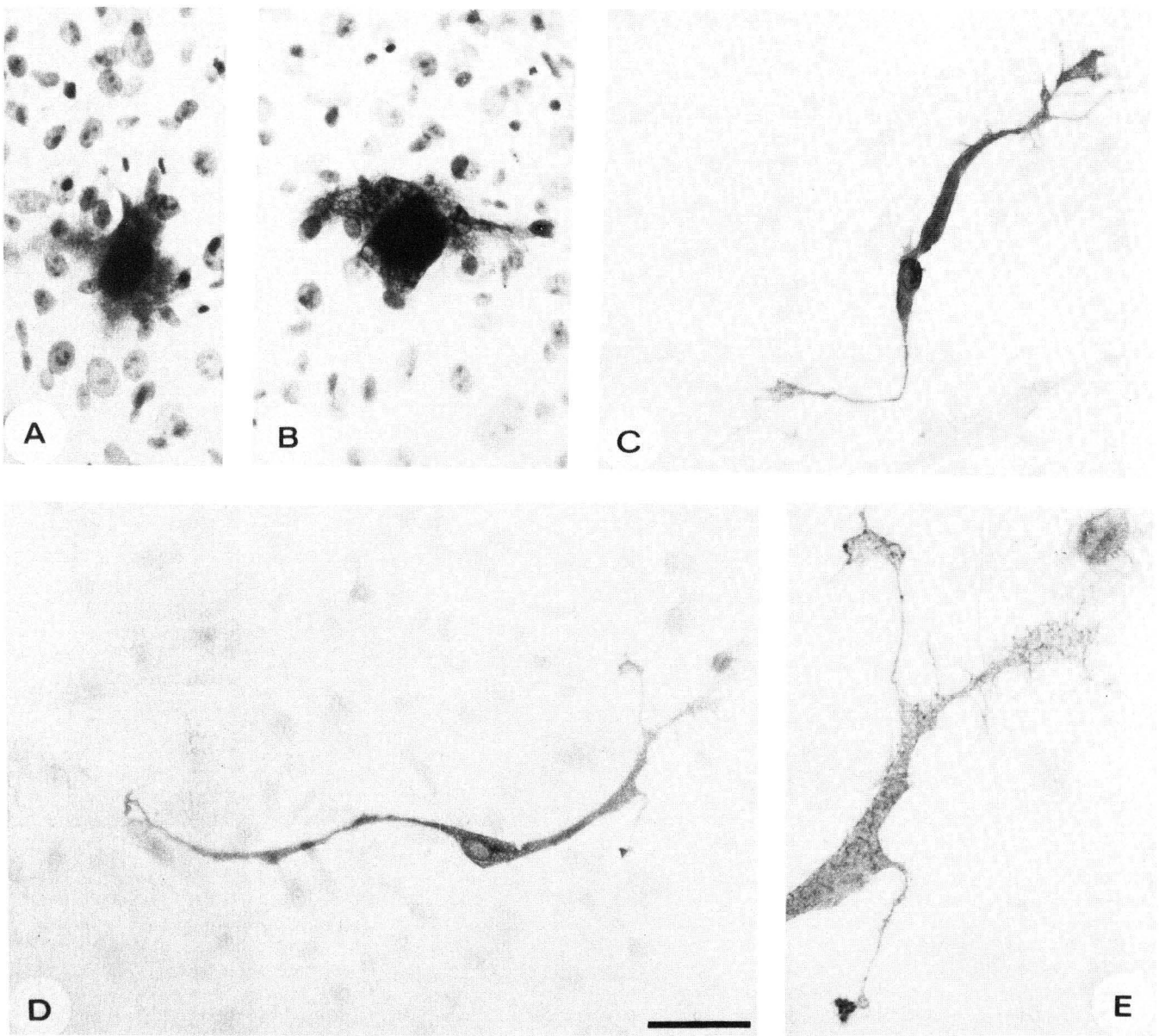

Fig. 5. Changes in the shape of rabbit skin cells expressing B-50/GAP-43. Rabbit skin cells expressing β-gal (A,B) and B-50/GAP-43 (C,D,E) 48 h after infection with dvHCL and dvHCB-50. Note the changes in cell shape in rabbit skin cells expressing B-50/GAP-43. E is a detail of the cell in D and illustrates multiple processes terminating in growth cone like structures. Bar = 50 μm for A–D and 19 μm for E.

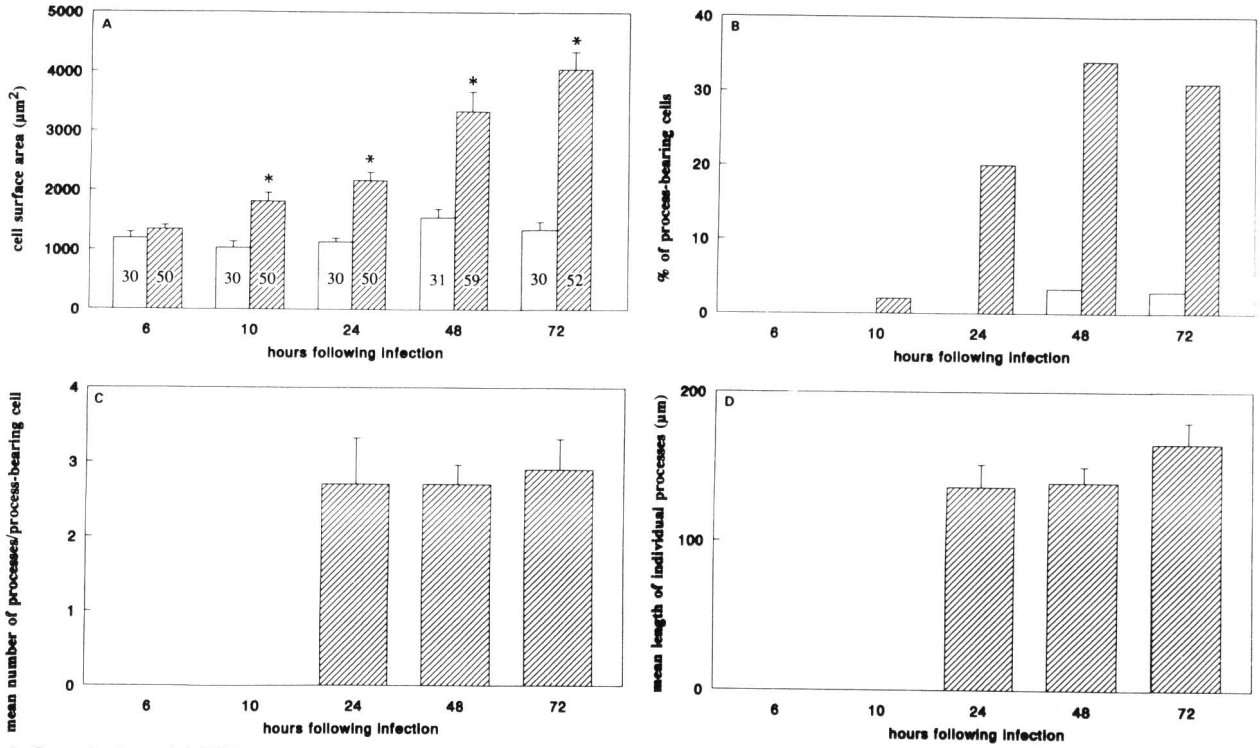

Fig. 6. Quantitation of dvHCL and dvHCB-50 infected vero cells at various times following infection. Vero cells cultured on poly-L-lysine-coated microscope slides were infected with dvHCL or dvHCB-50. Cells were fixed at 6, 10, 24, 48 and 72 h following infection and β-gal and B-50/GAP43-positive cells were identified with a histochemical staining (β-gal) or immunocytochemically (B-50/GAP-43) as detailed in the Materials and methods section. We determined the cell surface area (A), the percentage of process-bearing cells (B), the mean number of processes per process-bearing cell (C) and the mean length of individual processes (D) using a computerized image analyzer at 6, 10, 24, 48 and 72 h following infection with dvHCL (open bars) and dvHCB-50 (hatched bars). The numbers of cells analysed at each time point are indicated in the bars of A. Statistical analysis of the results was performed with a Student's *t*-test (* $P < 0.05$, dvHCL-infected cells versus dvHCB-50-infected cells).

with cell bodies of non-labelled cells and apparently preferred their surface as a matrix for elongation of their processes.

3.3. Quantitative analysis of B-50 / GAP-43-induced morphological changes

The changes in the shape of Vero cells were further analysed with an image analyser. We measured the cell surface area, the number of cells with one or more processes, the length of individual processes and the number of processes per process-bearing cell of 30 to 59 cells at each time point (Fig. 6). The surface area of the B-50/GAP43-positive cells increased gradually from 10 h up to 72 h post-infection (Fig. 6A). At 72 h, the B-50/GAP43-positive cells were 3.0 times larger in size as compared to the β-gal-expressing cells. B-50/GAP43-positive cells with processes were not observed at 6 h but started to appear between 10 and 24 h post-infection. At 72 h, 31% of the cells exhibited processes with a mean length of 165 ± 14.5 μm (Fig. 6B,D). The mean number of processes per process-bearing cell increased sharply from virtually no processes at 10 h following infection to 2.7 ± 0.6 processes per cell at 24 h following infection. The mean number of processes per process-bearing cell was retained between 24 and 72 h post-infection (Fig. 6C). Thus, the quantitative analysis of Vero cells shows that the B-50/GAP-43-positive cells become more complex over time and retain their changed morphology in culture for at least 72 h.

4. Discussion

The neural phosphoprotein B-50/GAP-43 has been associated with the formation of nerve fibers [41] and with the determination of cell shape [57]. A large body of circumstantial evidence indicates the involvement of B-50/GAP-43 in the development and regeneration of neuronal connections. One approach to demonstrating a direct effect of B-50/GAP-43 on cell shape and nerve fiber extension would be to create a gene transfer system that allows long-term high-level expression of the B-50/GAP-43 gene product in cells in culture and in vivo. As an initial and necessary step towards achieving this goal, we have generated a defective HSV vector containing the B-50/GAP-43 gene. These vec-

tors transfer and express the B-50/GAP-43 gene in cells in tissue culture. We demonstrate that B-50/GAP-43 expression in non-neuronal cells induces progressive changes in the shape of these cells eventually resulting in a considerable number of cells with a neuron-like morphology. This demonstrates that B-50/GAP-43 can initiate changes in cell shape and suggests a direct involvement of this growth-associated protein in the elaboration of cellular processes.

Our results differ in two important aspects from previously reported B-50/GAP-43-induced changes in cell shape [55,57]. First, the previous changes were quite modest as compared to the data presented here. For instance, transfection of a B-50/GAP-43 expression vector in COS cells [55] increased their cell surface area from 1000 μm^2 to 1340 μm^2, whereas we observed increases from 1342 μm^2 to 4044 μm^2 in Vero cells. Stably transfected CHO cell lines exhibited membrane ruffling and filopodial extensions of 20 to 75 μm in only 15% to 40% of the cells expressing B-50/GAP-43 [57]. We observed cell surface changes in virtually all cells expressing B-50/GAP-43. In addition, one third of these cells expressed processes with a mean length of 165 μm. This is more than twice as long as the longest filopodial extensions seen on CHO cells. Apparently, the introduction of B-50/GAP-43 in a cell provides this cell with a new function, i.e. the ability to enlarge its plasma membrane and form numerous long extensions. The predominant expression of B-50/GAP-43 on the plasma membrane of the extensions and the association of high levels of the protein with the formation of varicosities add strong support to a direct relationship between the elaboration of processes and the presence of B-50/GAP-43.

A second important difference between the previous cellular changes in response to B-50/GAP-43 and the current data lies in the timing of the effects. The previous morphological effects became manifest in the first 2 to 4 h following plating of the cells and were of a transient nature. In contrast, in cells expressing B-50/GAP-43 via a defective HSV vector, the cellular morphology gradually became more complex and the induced changes persisted up to 72 h in culture (Fig. 6). Although the differences in our results in Vero and rabbit skin cells and those seen in CHO and COS cells may be related to the differences in cell type used, we consider this only a formal possibility. COS cells are derived from CV-1 cells. CV-1 cells and Vero cells are both derived from African green monkey kidney cells. Thus, COS cells and Vero cells are very closely related cell types. Furthermore, our observations of similar effects in Vero and rabbit skin cells suggest that the morphological changes are not a cell type-specific phenomenon.

One suggestion raised by these differential effects of B-50/GAP-43 on cell shape is the influence of the level of expression of B-50/GAP-43 upon changes in cells shape. We did not make an attempt to quantify the amount of B-50/GAP-43 production in individual cells in culture. However, the polyclonal antibody used in this study was used at a higher dilution (1/2500) than usual in light microscopic studies on B-50/GAP-43 in brain sections (1/1000). At this higher dilution, most of the cells were darkly stained, indicating a high level of B-50/GAP-43 synthesis. The use of a strong viral promoter to drive gene expression, and transfer of the gene via a defective viral vector may have contributed to our observations. The CMV IE promoter is a very strong transcriptional activator [34] and each vector will package numerous copies of the plasmid genome up to 150 kb [42]. Each infected cell will therefore contain numerous copies of the B-50/GAP-43 transcription unit. Finally, gene transfer through viral infection results in greater uniformity of gene delivery than with transfection of naked DNA, in which the number of copies of a gene entering a cell can be quite variable. The defective HSV vector permits uniform gene transfer, which is one reason for creating a stably transfected cell line, and the vector also transfers multiple copies in an episomal form, thereby limiting the possibility of low gene expression due to insertional influences on the transgene. Thus, the dramatic and persistent cell surface reactions in virtually the total population of B-50/GAP-43-expressing cells may be related to the uniform high level of expression that can be achieved by defective herpes viral vector gene transfer.

The mechanism by which B-50/GAP-43 changes the shape of non-neuronal cells and causes the formation of long processes reminiscent of neurites is not clear. The shape of non-neuronal cells is affected by a number of factors such as the culture density, the phase of the cell cycle and the presence of mitogenic stimuli [7]. In neuronal cell lines as studied so far enhanced B-50/GAP-43 synthesis was not by itself sufficient to induce nerve fiber extensions [30,56]. Neurons are normally dependent on the presence of an appropriate differentiating agent that induces sprouting. Increased levels of B-50/GAP-43 in neuronal cell lines have been shown, however, to facilitate the sprouting response following the application of a growth factor [56] or retinoic acid [30]. A recently shown interaction between B-50/GAP-43 and G-proteins in growth-cone membrane preparations [43,44] and in *Xenopus laevis* oocytes [45] provides compelling evidence for a role of B-50/GAP-43 as an intracellular component in the control of receptor-mediated signal transduction. B-50/GAP-43 regulation of receptor-coupled G-proteins and its affinity for calmodulin [2,1] may be important in a molecular cascade eventually resulting in focal neuronal membrane addition, i.e. elaboration of nerve fibers. Non-neuronal cells do not normally respond to

stimuli like growth factors with the elaboration of long thin stable cellular processes as is the case in neurons. Thus, non-neuronal cells apparently lack the specific transduction systems that are operative in the control of nerve fiber growth in neurons. The introduction of B-50/GAP-43 in non-neuronal cells may result in the differential regulation of components of the signal transduction systems active in non-neuronal cells such as G-proteins. This could trigger a membrane response, as shown in the B-50/GAP-43-expressing non-neuronal cells in this paper, that has a striking resemblance to that seen in neurons during development or following neuronal damage.

In future studies, the herpes-based defective B-50/GAP-43 expression vector will be employed to investigate the effect of B-50/GAP-43 on the regenerative capacity of damaged neurons. Neurons of the adult mammalian central nervous system usually fail to regenerate following injury [41]. Although B-50/GAP-43 is induced in some CNS nerve cells following lesion, in close proximity to their cell bodies [12] increases in B-50/GAP-43 expression are relatively slow as compared to inductions in the PNS [47,54]. Thus, one of the factors that may contribute to the poor regeneration of injured central nervous system neurons may relate to the diminished capacity of these neurons to upregulate B-50/GAP-43. The expression of B-50/GAP-43 via a defective viral vector in damaged central nervous system neurons could potentially enhance their regenerative capacity. In addition, other regeneration-related proteins could be expressed with this vector system in vivo to explore their beneficial effect in nervous tissue regeneration.

Acknowledgements

This work was supported by NWO-MW Grant 900-521-121. J.V. is a fellow of the Royal Netherlands Academy of Arts and Sciences.

References

[1] Alexander, K.A., Wakim, B.T., Doyle, G.S., Walsh, K.A. and Storm, D.R., Identification and characterization of the calmodulin binding domain of neuromodulin, a neurospecific calmodulin-binding protein, *J. Biol. Chem.*, 263 (1988) 7044–7049.

[2] Andreason, T.J., Luetje, C.W., Heideman, D.R. and Storm, D.R., Purification of a novel calmodulin-binding protein from bovine cerebral cortex membranes, *Biochemistry*, 22 (1983) 4615–4623.

[3] Burry, W.B., Lah, J.J. and Hayes, D.M., Redistribution of GAP-43 during growth cone development in vitro: immunocytochemical studies, *J. Neurocytol.*, 21 (1991) 413–425.

[4] Basi, G.S., Jacobson, R.D., Virag, I., Schilling, J. and Skene, J.P.H., Primary structure and regulation of GAP-43, a protein associated with nerve growth, *Cell*, 49 (1987) 785–791.

[5] Benowitz, L.I., Shashoua, V.E. and Yoon, M.G., Specific changes in rapidly transported proteins during regeneration of the goldfish optic nerve, *J. Neurosci.*, 1 (1981) 300–307

[6] Biffo, S., Verhaagen, J., Schrama, L.H., Schotman, P., Danho, W. and Margolis, F.L., B-50/GAP-43 expression correlates with process outgrowth in the embryonic mouse nervous system, *Eur. J. Neurosci.*, 2 (1990) 487–499.

[7] Burgess, T.L. and Kelly, R.B., Constitutive and regulated secretion of proteins, *Annu. Rev. Cell Biol.*, 3 (1987) 243–293.

[8] Caceras, A., Mautino, J. and Kosik, K.S., Suppression of MAP2 in cultured cerebeller macroneurons inhibits minor neurite formation, *Neuron*, 9 (1992) 607–618.

[9] Cimler, B.M., Giebelhaus, D.H., Wakim, B.T., Storm, D.T. and Moon, R.T., Characterization of murine cDNAs encoding P-57, a neural-specific calmodulin-binding protein, *J. Biol. Chem.*, 262 (1987) 12158–12163.

[10] Coggins, J.C. and Zwiers, H., Evidence for a single protein kinase C-mediated phosphorilation site in rat brain protein B-50, *J. Neurochem.*, 56 (1989) 1095–1106.

[11] De Graan, P.N.E., Van Hooff, C.O.M., Tilly, B.C., Oestreicher, A.B., Schotman, P. and Gispen, W.H., Phosphoprotein B-50 in neuronal growth cones from fetal rat brain, *Neurosci. Lett.*, 61 (1985) 235–241.

[12] Doster, S.K., Lozano, A.M., Aguano, A.J. and Willard, W.B., Expression of the growth-associated protein GAP-43 in adult rat retinal ganglion cells following axon injury, *Neuron*, 6 (1991) 635–647.

[13] Easter, S.S., Ross, L.S. and Frankfurther, A., Initial tract formation in the mouse brain, *J. Neurosci.*, 13 (1993) 285–299.

[14] Federoff, H.J., Geschwind, M.D., Geller, A.I. and Kessler, J.A., Expression of nerve growth factor in vivo from a defective herpes simplex virus 1 vector prevents effects of axotomy on sympathetic ganglia, *Proc. Natl. Acad. Sci. USA*, 89 (1992) 1636–1640.

[15] Geller, A.I. and Breakefield, X., A defective HSV-1 vector expresses *Escherichia coli* beta-galactosidase in cultured peripheral neurons, *Science*, 241 (1988) 1667–1669.

[16] Goslin, K., Schreyer, D.J., Skene, J.P.H. and Banker G., Development of neuronal polarity: GAP-43 distinguishes axonal from dendritic growth cones, *Nature*, 336 (1988) 672–674.

[17] Ho, D.Y., Mocarski, E.S. and Sapolsky, R.M., Altering central nervous sustem physiology with a defective herpes simplex virus expressing the glucose reporter gene, *Proc. Natl. Acad. Sci. USA*, 90 (1993) 3655–3659.

[18] Hoffman, P.N., Expression of GAP-43, a rapidly transported growth-associated protein, and class 2 beta tubilin, a slowly transported cytoskeletal protein, are coordinated in regenerating neurons, *J. Neurosci.*, 9 (1989) 893–897.

[19] Jap Tjoen San, E.R.A., Schmidt-Michels, M., Oestreicher, A.B., Gispen, W.H. and Schotman, P., Inhibition of B-50/GAP-43 expression by antisense oligomers interferes with neuronal outgrowth, *Biochem. Biophys. Res. Commun.*, 187 (1992) 839–846.

[20] Katz, F., Ellis, L. and Pfenninger, K.H., Nerve growth cones isolated from fetal rat brain III calcium-dependent protein phosphorylation, *J. Neurosci.*, 5 (1985) 1402–1411.

[21] Kaplitt, M.G., Pfaus, J.G., Kleopoulos, S.P., Hanlon, B.A., Rabkin, S.D. and Pfaff, D.W., Expression of a functional foreign gene in adult mammalian brain following in vivo transfer via a Herpes Simplex virus Type 1 defective vector, *Mol. Cell. Neurosci.*, 2 (1991) 320–330.

[22] Kaplitt, M.G., Kwong, A., Kleopoulos, S.P., Rabkin, S.D. and Pfaff, D.W., *Proc. Natl. Acad. Sci. USA*, in press.

[23] Kristjansson, G.I., Zwiers, H., Oestreicher, A.B. and Gispen, W.H., Evidence that the synaptic phosphoprotein B-50 is localized exclusively in nerve tissue, *J. Neurochem.*, 39 (1982) 371–378.

[24] Kumagai, C., Tohda, M., Isobe, M. and Nomura, Y., Involve-

ment of growth-associated protein-43 with irreversible neurite outgrowth by dibutyryl cyclic AMP and phorbol ester in NG108–15 cells, *J. Neurochem.*, 59 (1992) 41–47.

[25] Kwong, A.D. and Frenkel, N. Herpes simplex virus amplicon: effect of size on replication of constructed defective genomes containing eukaryotic DNA sequences, *J. Virol.*, 51 (1984) 595–603.

[26] Lewis, A.K. and Bridgman, P.C., Nerve growth cone lamellipodia contain two populations of actin filaments that differ in organization and polarity, *J. Cell Biol.*, 119 (1992) 1219–1243.

[27] Lewis, S.A., Ivanov, I.E., Lee, G.H. and Cowan, N.J., Organisation of microtubules in dendrites and axons is determined by a short hydrophobic zipper in microtubule-associated proteins MAP-2 and tau, *Nature*, 342 (1989) 498–505.

[28] Miller, F.D., Tetzlaff, W., Bisby, M.A., Fawcett, J.W. and Milner, R.J.,. Rapid induction of the major embryonic α-tubilin mRNA, in adults following neuronal injury, *J. Neurosci.*, 9 (1989) 1452–1463.

[29] Nielander, H.L., Schrama, L.H., Van Rozen, A.J., Kasperaitis, M., Oestericher, A.B., De Graan, P.N.E., Gispen, W.H. and Schotman, P., Primary structure of the neuron-specific phosphoprotein B-50 is identical to growth-associated protein GAP-43, *Neurosci. Res. Commun.*, 1 (1987) 163–172.

[30] Morton, A.J. and Buss, T.N., Accelerated differentiation in response to Retinoic Acid after retrovirally mediated gene transfer of GAP-43 into mouse neuroblastoma cells, *Eur. J. Neurosci.*, 4 (1992) 910–916

[31] Oestreicher, A.B., Van Dongen, C.J., Zwiers, H. and Gispen, W.H., Affinity-purified anti-B-50 protein antibody: Interference with the function of the phosphoprotein B-50 in synaptic plasma membranes, *J. Neurochem.*, 41, 331–340.

[32] Rosenthal, A., Chan, S.Y., Henzel, W., Haskell, C., Kuang, W.-J., Chen, J.N., Wilcox, A., Ullrich, D.V., Goeddel, E. and Routtenberg, A., Primary structure and mRNA localization of protein F1, a growth-related protein kinase C substrate associated with synaptic plasticity, *EMBO J.*, 6 (1987) 3611–6346.

[33] Sambrook, J., Fritsch, E.F. and Maniatis, T., In: *Molecular Cloning. A Laboratory Manual*, 2nd edn., Cold Spring Harbor Laboratory Press, New York, 1989.

[34] Scharfmann, R., Axelrod, J.H. and Verma, I.M., Long-term in vivo expression of retrovirus-mediated gene transfer in mouse fibroblast implants, *Proc. Natl. Acad. Sci. USA*, 88 (1991) 4626–4630.

[35] Shirao, T., Kojima, N. and Obata, K., Cloning of drebrin A and induction of neurite-like processes in drebrin-transfected cells, *NeuroReport*, 3 (1992) 109–112.

[36] Shea, T.B., Perrone-Bizzozero, N.I., Beerman, M.L. and Benowitz, L.I., Phospholipid-mediated delivery of anti-GAP-43 antibodies into neuroblastoma cells prevents neuritogenesis, *J. Neurosci.*, 11 (1991) 1685–1690.

[37] Skene, J.P.H. and Willard, M., Axonally transported proteins associated with axon growth in rabbit central and peripheral nervous system, *J. Cell Biol.*, 89 (1981) 96–103.

[38] Skene, J.P.H. and Willard, M., Changes in axonally transported proteins during axonal regeneration in toad retinal ganglion cells, *J. Neurosci.*, 1 (1981) 419–426.

[39] Skene, J.P.H., Jacobson, R.D., Snipes, G.J., McGuire, C.B., Norden, J.I. and Freeman, J.A., A protein induced during nerve growth (GAP-43) is a major component of growth cone membranes, *Science*, 233 (1986) 783–786.

[40] Skene, J.P.H., Axonal growth associated proteins, *Annu. Rev. Neurosci.*, 12 (1989) 127–156.

[41] Skene, J.P.H., Retrograde pathways controlling expression of a major growth cone component in the adult CNS. In Letourneau, P.C., Kater, S.B. and Macagno, E.R. (Eds.), *The Nerve Growth Cone*, 1989.

[42] Speate, R.R. and Frenkel, N., The herpes simplex virus amplicon: A new eukaryotic defective-virus cloning-amplifying vector, *Cell*, 30 (1982) 295–304.

[43] Strittmatter, S.M., Valenzuela, D., Kennedy, T.E., Neer, E.J. and Fishman, M.C., G_0 is a major growth cone protein subject to regulation by GAP-43, *Nature*, 344 (1990) 836–841.

[44] Strittmatter, S.M., Valenzuela, D., Sudo, Y., Linder, M.E. and Fishman, M.C., An intracellular guanine nucleotide release protein for G_0, *J. Biol. Chem.*, 266 (1991) 22465–22471.

[45] Strittmatter, S.M., Cannon, S.C., Ross, E.M., Higashijima, T. and Fishman, M.C., GAP-43 augments G-protein coupled receptor transduction in X. laevis oocytes, *Proc. Natl. Acad. Sci. USA*, 90 (1993) 5327–5331.

[46] Tetzlaff, W. and Bisby, M.A., *Rest. Neurol. Neurosci.*, 1 (1990) 189–196.

[47] Tetzlaff, W., Alexander, S.W., Miller, F.D. and Bisby, M.A., Response of facial and rubrospinal neurons to axotomy: changes in mRNA expression for cytoskeletal proteins and GAP-43, *J. Neurosci.*, 11 (1991) 2528–2544.

[48] Towbin, H., Steahelin, T. and Gordon, J., Electrophoretic transfer of proteins from polyacrylamide gels to nitrocellulose sheets: procedure and application, *Proc. Natl. Acad. Sci. USA*, 76 (1984) 4354–4356.

[49] Van der Zee, C.E.E.M., Nielander, H.B., Vos, J.P., Lopes da Silva, S., Verhaagen, J., Oestreicher, A.B., Schrama, L.H., Schotman, P. and Gispen, W.H., Expression of growth-associated protein B-50 (GAP-43). in dorsal root ganglia and the sciatic nerve during regenerative sprouting, *J. Neurosci.*, 9 (1989) 3505–3512.

[50] Van Lookeren-Campagne, M, Dotti, C.G., Jap Tjoen San, E.R.A., Verkley, A.J., Gispen, W.H. and Oestreicher, A.B., B-50/GAP-43 localization in polarized hippocampal neurons in vitro: an ultrastructural quantitative study, *Neuroscience*, 50 (1992) 35–52.

[51] Van Hooff, C.O.M., Holthuis, J.C.M., Oestreicher, A.B., Boonstra, J., De Graan, P.N.E. and Gispen, W.H., Nerve growth factor induced changes in the intracellular localization of the protein kinase C substrate B-50 in pheochromacytoma cells, *J. Cell Biol.*, 108 (1989) 1115–1125.

[52] Verhaagen, J., Van Hooff, C.O.M., Edwards, P.M., De Graan, P.N.E., Oestreicher, A.B., Schotman, P., Jennekens, F.G.I. and Gispen, W.H., The kinase C substrate protein B-50 and axonal regeneration, *Brain Res. Bull.*, 17 (1986) 737–741.

[53] Verhaagen, J., Oestreicher, A.B., Edwards, P.M., Veldman, H., Jennekens, F.G.I. and Gispen, W.H., Light and electron microscopical study B-50 following denervation and reinnervation of the rat soleus muscle, *J. Neurosci.*, 8 (1988) 1759–1766.

[54] Verhaagen, J., Zhang, Y., Hamers, F.P.T. and Gispen, W.H., Elevated expression of B-50(GAP-43)-mRNA in a subpopulation of olfactory bulb mitral cells following axotomy, *J. Neurosci. Res.*, 35 (1993) 162–169.

[55] Widmer, F. and Caroni, P., Phosphorylation-site mutagenesis of the growth-associated protein GAP-43 modulates its effect on cell spreading and morphology, *J. Cell Biol.*, 120 (1993) 503–512.

[56] Yankner, G.A., Benowitz, L.I., Villa Kamoroff, L. and Neve, R.L., Transfection of PC-12 cells with the human GAP-43 gene: effects on neurite outgrowth and regeneration, *Mol. Brain Res.*, 7 (1990) 39–44.

[57] Zuber, M.X., Goodman, D.W., Karns, L.R. and Fishman M.C., The neuronal growth-associated protein GAP-43 induces filopodia in non-neuronal cells, *Science*, 244 (1989) 1193–1195.

[58] Zwiers, H., Veldhuis, H.D., Schotman, P. and Gispen, W.H., Cyclic nucleotides, and brain protein phosphorylation in vitro, *Neurochem. Res.*, 1 (1976) 669–677.

[59] Zwiers, H., Schotman, P. and Gispen, W.H., Purification and some characteristics of an ACTH-sensitive protein kinase and its substrate protein in rat brain membranes, *J. Neurochem.*, 34 (1980) 1689–1699.